A STUDY OF HEATED FREE JETS OF CIRCULAR CROSS SECTION

B. Hanel and B. Weidemann

UDC 532.525.2

We propose simple formulas based on experimental data derived for temperature and velocity fields in heated free jets of circular cross section, discharging horizontally out of a circular nozzle or directed vertically downward.

Comparison of methods to calculate nonisothermal free jets demonstrates that the choice of the various empirical quantities may produce significant differences in the characteristics of propagation and attenuation, which may not be neglected in engineering practice. These calculation methods have therefore been subjected to verification, and various correction factors have been introduced on the basis of results from direct experimental research in which the data of other authors have been taken into consideration. We have investigated a heated free jet of circular cross section being discharged horizontally or straight down.

In the range $10^2 < Re_0 < 2 \cdot 10^4$ and $0 < Ar_0 < 10^{-1}$ we have determined experimentally the following free-jet characteristics: trajectory, change in velocity and temperature along the axis in the case of horizontal discharge; depth of penetration in vertical flow; distribution of temperatures and velocities through the cross section of the jet; turbulent fluctuations in temperature and velocity.

In the following we present but a few of the most important results, with additional information available in [1-3, 7].

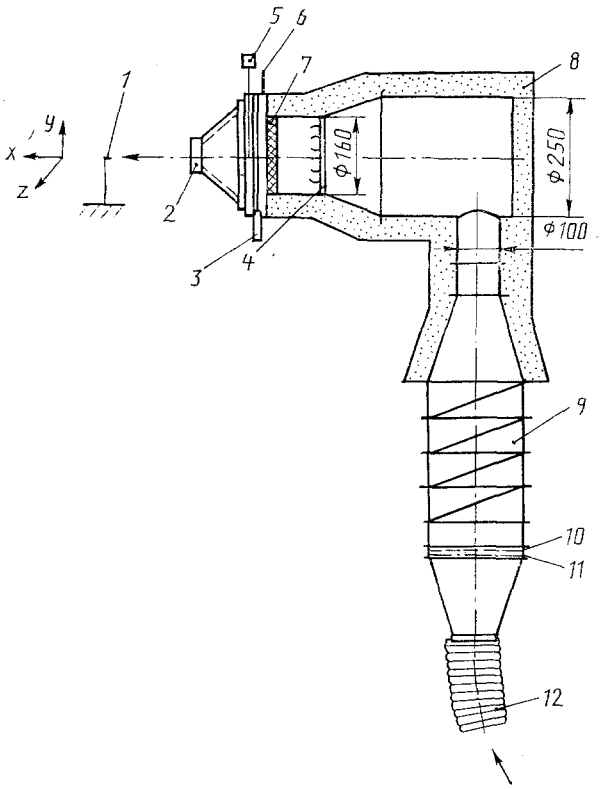

Fig. 1. Diagram showing preparation and supply of air: 1) sensing element for temperature and velocity measurements; 2) ceramic nozzle; 3) smoke inlet for qualitative tests; 4) flow equalization nozzle; 5) thermocouple in shielded shell; 6) pressure measurement terminal; 7) porous metal; 8) insulation; 9) electrical heating 4 × 1 kW (continuously controlled); 10) metal sieve; 11) Fiberglas material; 12) connection to centrifugal fan.

Technical University, Dresden. Translated from Inzhenerno-Fizicheskii Zhurnal, Vol. 60, No. 3, pp. 393-401, March, 1991. Original article submitted July 31, 1989.

0022-0841/91/6003-0310$12.50

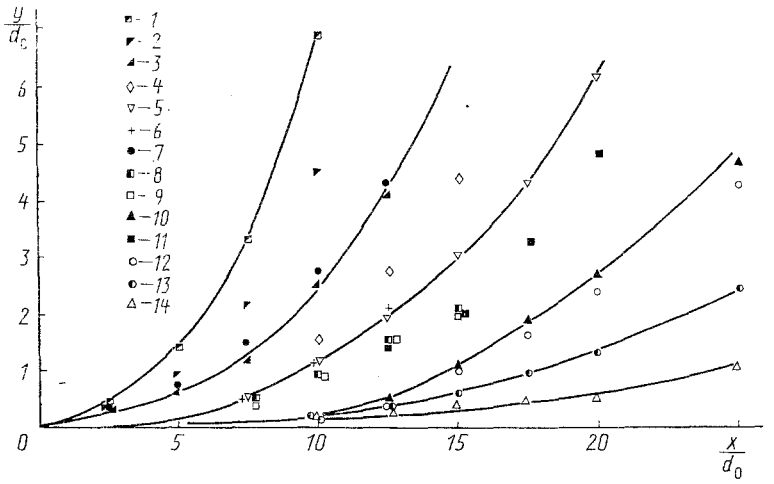

Fig. 2. Free-jet horizontal discharge trajectories: 1) $Ar_0 = 7.36 \cdot 10^{-2}$, $Re_0 = 2.5 \cdot 10^3$; 2) $4.86 \cdot 10^{-2}$ and $0.91 \cdot 10^4$; 3) $2.12 \cdot 10^{-2}$ and $1.21 \cdot 10^4$; 4) $1.46 \cdot 10^{-2}$ and $5.82 \cdot 10^3$; 5) $1.34 \cdot 10^{-2}$ and $5.99 \cdot 10^3$; 6) $1.14 \cdot 10^{-2}$ and $6.8 \cdot 10^3$; 7) $0.99 \cdot 10^{-2}$ and $1.95 \cdot 10^3$; 8) $8.9 \cdot 10^{-3}$ and $7.5 \cdot 10^3$; 9) $8.5 \cdot 10^{-3}$ and $7.8 \cdot 10^3$; 10) $6.25 \cdot 10^{-3}$ and $0.91 \cdot 10^4$; 11) $5.32 \cdot 10^{-3}$ and $2.56 \cdot 10^3$; 12) $3.0 \cdot 10^{-3}$ and $1.34 \cdot 10^4$; 13) $1.76 \cdot 10^{-3}$ and $1.58 \cdot 10^3$; 14) $4.95 \cdot 10^{-4}$ and $0.86 \cdot 10^4$.

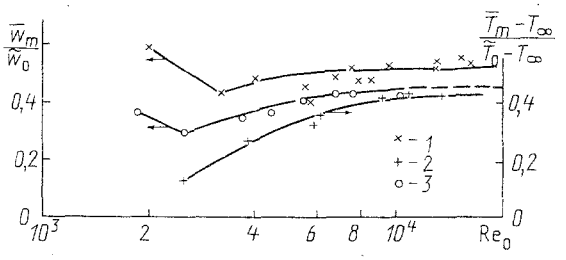

Fig. 3. Velocity and temperature at the axis of horizontally discharged free jets of circular cross section (Gr_0 = const) as functions of $Re_0(x/d_0 = 10)$: 1, 2) $Gr_0 \approx 50 \cdot 10^4$; 3) $4 \cdot 10^4$.

Experimental Installation and Measurement Techniques. Figure 1 shows a diagram of the experimental installation for research into horizontal free jets. A centrifugal fan is used to draw in air at an ambient temperature of $T_\infty \approx 20°C$. The air flow passes over the heating segment and on turning through 90° reaches the mixing chamber which contains a variety of devices (a mixing nozzle, porous metal), which ensure excellent mixing and homogenization of the hot air ($T_{0,max} \approx 250°C$). Ceramic nozzles similar to nozzles used in wind tunnels (d_0 = 20, 47, and 92 mm) serve as the outlet elements. Because of the adopted nozzle profile, the above-cited devices, in addition to thorough insulation of the experimental installation, we were able to achieve outlet temperatures very nearly rectangular in profile. In order to study the vertical free jets, we rotated this same installation (Fig. 1) through 90°.

The devices in the mixing chamber produced in these experiments a comparatively high level of turbulence in the nozzle outlet ($Tu_0 \approx$ 3-5%), as a consequence of which the length of the free-jet core could be reduced approximately to $1\text{-}2d_0$.

Measurement of the average velocities and temperatures, as well as of the fluctuations in temperature and velocity, were performed with the aid of a DISA-55M system. Since the experiments encompassed a comparatively broad range of temperatures, we had to employ a variety of measurement methods. Up to outlet temperatures of $T_0 \approx 120°C$ the mean velocities were determined with the aid of a 55M14 measuring bridge with temperature compensation, combined with 55E30 and 55P86 probes (the diameter of the heating filament was 5 μm). At higher air temperatures, we used the 55M10 measuring bridge with a high-temperature 55A74-type probe (the diameter of the heating filament is 9 μm). For purposes of measuring fluctuations in temperature and velocity we had to use probes with excellent dynamic characteristics (2.5 μm). For purposes of determining the average temperatures, we used both probes with a heating filament (5 μm) and thermocouples in shielded containers.

In all of the measurements, the positions of the probes were established in a nonmoving space-oriented Cartesian coordinate system. Such an approach is not always correct in investigating horizontal discharge of a nonisothermal free jet. Precise determination of the axis of the free jet is possible only in measurements perpendicular to the latter. In this case, however, we would have to employ cumbersome repeated measurements. It has been established that with slight curvature in the axis of the free jet measurement through the vertical cross sections makes it possible to determine the axis with adequate accuracy. The relative errors $\Delta y/y > 10\%$

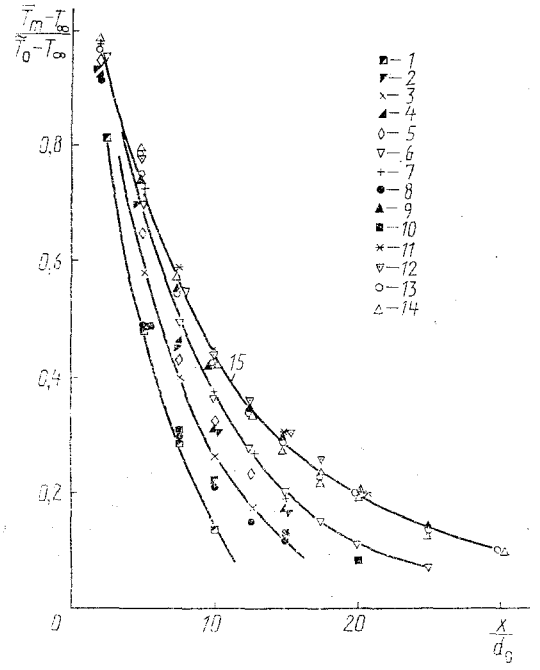

Fig. 4

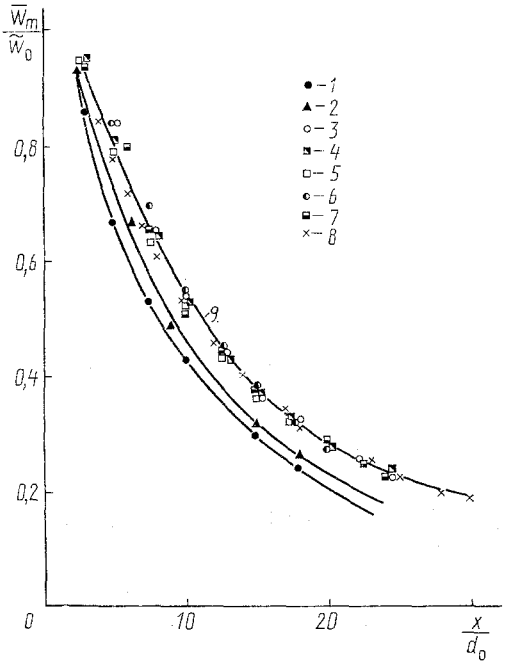

Fig. 5

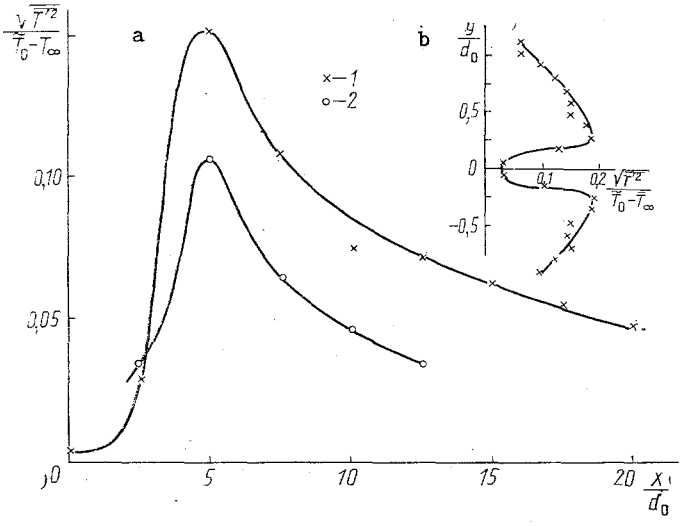

Fig. 6

Fig. 4. Change in temperature along the axis of horizontally discharged free jets: 1) $Ar_0 = 7.36 \cdot 10^{-2}$, $Re_0 = 2.5 \cdot 10^3$; 2) $4.86 \cdot 10^{-2}$ and $0.91 \cdot 10^4$; 3) $2.99 \cdot 10^{-2}$ and $3.9 \cdot 10^3$; 4) $2.12 \cdot 10^{-2}$ and $1.21 \cdot 10^4$; 5) $1.46 \cdot 10^{-2}$ and $5.82 \cdot 10^3$; 6) $1.34 \cdot 10^{-2}$ and $5.99 \cdot 10^3$; 7) $1.14 \cdot 10^{-2}$ and $6.8 \cdot 10^3$; 8) $0.99 \cdot 10^{-2}$ and $1.95 \cdot 10^3$; 9) $6.25 \cdot 10^{-3}$ and $9.1 \cdot 10^3$; 10) $5.32 \cdot 10^{-3}$ and $2.56 \cdot 10^3$; 11) $4.41 \cdot 10^{-3}$ and $1.05 \cdot 10^4$; 12) $4.15 \cdot 10^{-3}$ and $1.08 \cdot 10^4$; 13) $3.0 \cdot 10^{-3}$ and $1.34 \cdot 10^4$; 14) $4.95 \cdot 10^{-4}$ and $8.6 \cdot 10^3$; 15) limit curve ($Ar_0 < 10^{-2}$, $Re_0 > 8 \cdot 10^3$).

Fig. 5. Change in velocity along the axis of horizontally discharged free jets: 1) $Ar_0 = 5.45 \cdot 10^{-2}$, $Re_0 = 8.34 \cdot 10^3$; 2) $3.03 \cdot 10^{-2}$ and $1.02 \cdot 10^4$; 3) $4.81 \cdot 10^{-3}$ and $9.87 \cdot 10^3$; 4) $2.85 \cdot 10^{-3}$ and $1.30 \cdot 10^4$; 5) $2.82 \cdot 10^{-3}$ and $1.30 \cdot 10^4$; 6) $1.76 \cdot 10^{-3}$ and $1.58 \cdot 10^4$; 7) $1.68 \cdot 10^{-3}$ and $1.63 \cdot 10^4$; 8) 0 and $1.86 \cdot 10^4$; 9) limit curve ($Ar_0 < 10^{-2}$, $Re_0 > 8 \cdot 10^3$).

Fig. 6. Fluctuating temperatures in a horizontally discharged free jet for the case in which $z/d_0 = 0$ (a, along the jet axis; b, perpendicular to that axis): 1) $Ar_0 = 4.7 \cdot 10^{-3}$ ($\tilde{T}_0 = 373$ K), $Re_0 = 1.02 \cdot 10^4$; 2) $Ar_0 = 3 \cdot 10^{-2}$ ($\tilde{T}_0 = 513$ K), $Re_0 = 3.9 \cdot 10^3$.

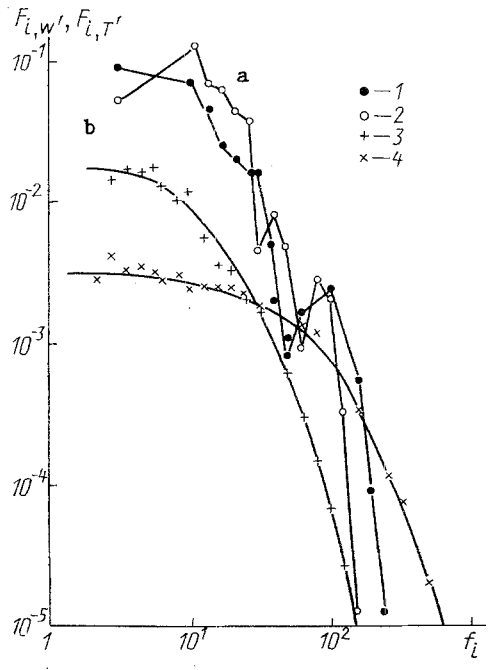

Fig. 7

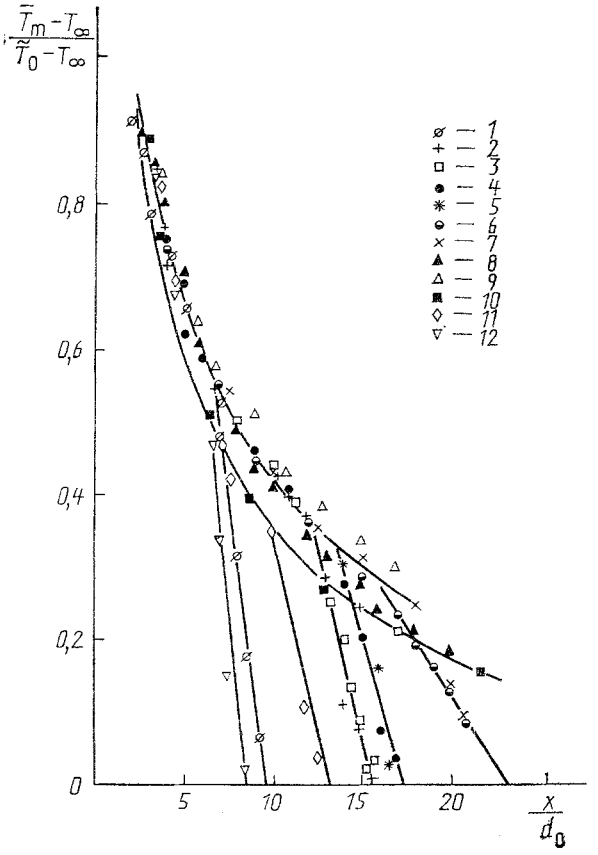

Fig. 8

Fig. 7. Spectra of turbulent quantities in a horizontally free jet: a) fluctuating velocities $\overline{w'^2}$ for $x/d_0 = 10$ (1: $Re_0 = 1.2 \cdot 10^4$, $Ar_0 = 3.6 \cdot 10^{-3}$; 2: $3.37 \cdot 10^3$ and $4.3 \cdot 10^{-2}$); b) fluctuating temperatures $\overline{T'^2}$ for $x/d_0 = 5$ [3: $Ar_0 = 8.6 \cdot 10^{-3}$ (T_0 = 476 K), $Re_0 = 2.1 \cdot 10^3$; 4: $2.6 \cdot 10^{-4}$ (434 K), and $1.24 \cdot 10^4$].

Fig. 8. Change in temperature along the axis of vertical free jets: 1) $Ar_0 = 2.7 \cdot 10^{-2}$, $Re_0 = 1.05 \cdot 10^4$; 2) $9.0 \cdot 10^{-3}$ and $7.2 \cdot 10^3$; 3) $8.7 \cdot 10^{-3}$ and $7.6 \cdot 10^3$; 4) $8.1 \cdot 10^{-3}$ and $7.5 \cdot 10^3$; 5) $7.9 \cdot 10^{-3}$ and $6.8 \cdot 10^3$; 6) $5.2 \cdot 10^{-3}$ and $9.0 \cdot 10^3$; 7) $4.9 \cdot 10^{-3}$ and $1.01 \cdot 10^4$; 8) $4.3 \cdot 10^{-3}$ and $1.05 \cdot 10^4$; 9) $3.5 \cdot 10^{-3}$ and $2.73 \cdot 10^3$; 10) $2.8 \cdot 10^{-3}$ and $3.85 \cdot 10^3$ [8]; 11) $1.94 \cdot 10^{-3}$ and $2.26 \cdot 10^3$ [8]; 12) $4.54 \cdot 10^{-2}$ and $1.54 \cdot 10^3$ [8].

in the determination of the free-jet axis arise only when the angle of the axis exceeds 60°. The corresponding error in the determination of a drop in temperature and velocity along the axis of the jet is less than 5%. For angles greater than 60° horizontally discharged free jets become buoyant. We did not investigate this type of free jet. It should also be noted that the space within which the free jets are propagated was shielded on three sides by means of movable barriers in order to exclude the effect of uncontrolled undesirable flows in the surrounding space on the measurement results.

A Horizontally Heated Free Jet of Circular Cross Section. Figure 2 shows that the free-jet axis is primarily governed by the Archimedes number. As Ar_0 increases, so does the deviation from the horizontal. However, one cannot regard the dependence on the Archimedes number as uniquely defined. Small Reynolds numbers ($Re_0 < 3000$: the region in which transition from laminar to turbulent flow takes place) lead to more pronounced trajectory curvature, since only when $Re_0 > 8 \cdot 10^3$ can we hold that the free jets have become completely turbulent (see Fig. 3 and [4, 6]).

Figure 4 shows the change in temperature along the axis of nonisothermal free jets. Even here we note the clear effect of the Archimedes number. As Ar_0 increases, so the reduction in temperature along the axis of the jet is accelerated. In the region of slight nonisothermicity ($Ar_0 < 10^{-2}$) at the same time, with clearly defined turbulence (high Reynolds numbers), we obtain the limit curve. In the region of transition from laminar to turbulent flow we may see the effect of Re_0 on the change in temperature. In measuring temperature fields we observed clear deformation of radial temperature distributions.

The curves showing the change in velocity along the axis (shown in Fig. 5) for completely turbulent free jets indicate that in a slightly nonisothermal free jet ($Ar_0 < 10^{-2}$) in analogy with the behavior of temperature fields, the measured points form the limit curve. At higher values of Ar_0 we observe a more rapid fall in velocity, owing to intensive turbulent transfer. At transition

from laminar to turbulent flow, the values of Ar_0 also significantly affect the reduction in velocity. However, here we have the imposition of the additional effect from the values of the Reynolds numbers.

Figure 6 shows fluctuations in temperature along the free-jet axis and in the direction perpendicular to it. At some distance too far removed from the nozzle outlet strong turbulent excitation is noted along the jet axis. At the end of the jet core the fluctuations in temperature relative to the temperature difference across the outlet attain their maximum values. The fluctuations are smaller at high temperatures than at low temperatures.

Turbulent fluctuations in temperature and velocity were measured in order to study free-jet structures (see Fig. 7). Unlike the spectral distributions of temperature fluctuations, in the one-dimensional frequency spectra of velocity fluctuations we encounter peaks in the inertial subregion ($f_i \approx$ 10-100 Hz), which point to the presence of discrete vortical configurations typical of transition regions. However, for the moment we have been unable to detect any significant role for the Reynolds number.

The theoretical formulas ($Re_0 > 8 \cdot 10^3$) are as follows:

for the trajectory

$$\frac{y}{d_0} = 0{,}08\, Ar_0 \left(\frac{x}{d_0}\right)^3;$$

for temperature measurements along the jet axis:

$$\frac{T_m - T_\infty}{T_0 - T_\infty} = 4{,}2\,\frac{d_0}{x}, \quad 6 < \frac{x}{d_0} < 15, \quad Ar_0 < 10^{-2};$$

$$\frac{T_m - T_\infty}{T_0 - T_\infty} = 5{,}6\,\frac{d_0}{x}\left(1 - 0{,}015\,\frac{x}{d_0}\right), \quad \frac{x}{d_0} > 15, \quad Ar_0 < 10^{-2};$$

$$\frac{T_m - T_\infty}{T_0 - T_\infty} = 5{,}1\,\frac{d_0}{x}\left(1 - 0{,}2\,\sqrt{Ar_0}\,\frac{x}{d_0}\right), \quad \frac{x}{d_0} > 6, \quad Ar_0 \geqslant 10^{-2};$$

for changes in velocity along the jet axis:

$$\frac{w_m}{w_0} = 5{,}6\,\frac{d_0}{x}, \quad \frac{x}{d_0} > 10, \quad Ar_0 < 10^{-2};$$

$$\frac{w_m}{w_0} = (5{,}6 - 25\,Ar_0)\,\frac{d_0}{x}, \quad \frac{x}{d_0} > 6, \quad Ar_0 \geqslant 10^{-2}.$$

Vertically Directed Heated Free Jet of Circular Cross Section. From the diagram showing the changes in temperature along the axis of the free jet (Fig. 8) we can see that here, in contrast to the case of horizontally discharged air, in the region near the nozzle all of the measurement-derived data come together in a very narrow band. We observe no dependence on the values of the Archimedes number. It is obvious that the predominance of the force of inertia over the force of buoyancy is characteristic of this region. The dimensionless length x/d_0 of this free-jet segment depends on Ar_0. The end of the segment is identified by a pronounced bend in the curve of temperature change. As Ar_0 increases, it shifts in the direction of shorter lengths. Near the bend in the curve showing the changes in temperature the end of the free jet is rapidly reached (disappearance). Theoretically one would expect a discontinuous drop to the temperature of the ambient medium. Fluctuations in the depth of penetration, however, lead to the difference (shown in Fig. 8) between the theoretically and experimentally derived temperature curves along the jet axis.

Figure 9 shows the predominant effect of the Archimedes numbers on the change in velocity along the axis of the jet. As Ar_0 increases, the velocity diminishes all the more rapidly. It is noteworthy that even at low Archimedes numbers ($Ar_0 \approx 10^{-3}$) we note a clear effect on the reduction in velocity. The extreme curve obtained for the case of a slightly nonisothermal horizontal free jet ($Ar_0 < 10^{-2}$) does not show up here. And we were unable to observe any effect from the Reynolds number with the spectral analysis method for the range ($Re_0 > 3000$). The depths of penetration x_{max}, derived from measurements of both temperatures and velocities, are in good agreement. Results from the measurements of fluctuations in temperature are comparable with the data derived for the case of a horizontal free jet, i.e., the quantity $\sqrt{\overline{T'^2}}(T_0 - T_\infty)$ increases rapidly to values of 0.1 when $x/d_0 \approx$ 4, and then drops off approximately 0.03 when $x/d_0 \approx 15$.

The theoretical formulas ($Re_0 > 3 \cdot 10^3$, $Ar_0 < 10^{-2}$), see also [9], are as follows:

for the depth of penetration,

$$x_{max} = 1{,}6\, d_0 / \sqrt{Ar_0};$$

for the change in temperature along the jet axis,

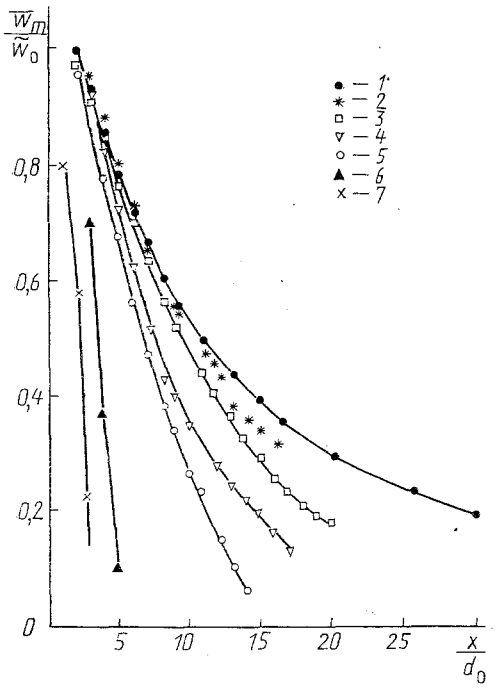

Fig. 9. Change in velocity along the axis of vertical free jets: 1) $Ar_0 = 0$, $Re_0 = 1.86 \cdot 10^4$; 2) $1.3 \cdot 10^{-3}$ and $1.7 \cdot 10^4$; 3) $2.77 \cdot 10^{-3}$ and $1.27 \cdot 10^4$; 4) $4.85 \cdot 10^{-3}$ and $1.04 \cdot 10^4$; 5) $9.5 \cdot 10^{-3}$ and $0.71 \cdot 10^4$; 6) $3.0 \cdot 10^{-2}$ and $9.1 \cdot 10^3$; 7) $6.2 \cdot 10^{-2}$ and $5.0 \cdot 10^3$.

$$\frac{T_m - T_\infty}{T_0 - T_\infty} = 4{,}2\,\frac{d_0}{x}, \quad 6 < \frac{x}{d_0} < 15;$$

$$\frac{T_m - T_\infty}{T_0 - T_\infty} = 5{,}6\,\frac{d_0}{x} - 0{,}085, \quad \frac{x}{d_0} \geqslant 15;$$

for the change in velocity along the jet axis

$$\frac{w_m}{w_0} = 5{,}6\,\frac{d_0}{x} - \left[3\,\mathrm{Ar}_0^{1{,}5}\left(\frac{x}{d_0}\right)^2 - 4\,\mathrm{Ar}_0\,\frac{x}{d_0} + 3{,}5\,\mathrm{Ar}_0^{0{,}25}\right], \quad \frac{x}{d_0} > 6.$$

The formulas derived from extensive experimental material presented in [1, 7], despite some formal differences, correspond well to the relationships presented in [5].

NOTATION

Ar_0, Archimedes number for the air at the outlet; $Ar_0 = gd_0(\tilde{T}_0 - T_\infty)/T_\infty \tilde{w}_0^2$; d_0, nozzle outlet diameter; g, acceleration of the force of gravity; $F_{i,T}$, spectrum of fluctuating velocities; f_i, mean frequency of the frequency band under consideration; Gr_0, Grasshof number for the air at the outlet, $Gr_0 = gd_0^2(\tilde{T}_0 - T_\infty)/T_\infty \nu_0^2$; Re_0, Reynolds number for the air at the outlet, $Re_0 = \tilde{w}_0 d_0/\nu_0$; $\bar{T}_m$, time-averaged temperature at the jet axis; $\tilde{T}_0$, outlet air temperature averaged over time and cross section; T_∞, temperature of the ambient medium; $\sqrt{\overline{T'^2}}$, mean square magnitude of temperature of fluctuations; $\bar{w}_m$, time-averaged velocity at the jet axis; $\tilde{w}_0$, outlet air velocity averaged over time and cross section; x, y, and z, coordinates; x_{max}, depth of penetration; ν_0, kinematic viscosity of the air at the outlet from the nozzle.

LITERATURE CITED

1. B. Weidemann, "Untersuchungen zum Verhalten horizontal und vertikal nach unten ausströmender runder warmer Freistrahlen," Dissertation, Technische Universität Dresden (1987).
2. B.Weidemann, B. Hanel, and G. Höppner, *Luft- und Kältetchnik*, **21**, No. 4, 214-233 (1985).
3. B. Hanel, H. Höppner, E. Richter, and B. Weidemann, *Wiss. Z. Techn. Univers. Dresden*, **35**, No. 4, 63-68 (1986).
4. B. Hanel and E. Richter, *Luft- und Kältetchnik*, **15**, No. 1, 12-17 (1979).
5. G. N. Abramovich (ed.), *The Theory of Turbulent Jets* [Russian translation], Moscow (1984).

6. L. A. Vulis, V. T. Zhivov, O. A. Kuznetsov, and L.P. Yarin, *Inzh.-Fiz. Zh.*, **21**, No. 1, 58-62 (1971).
7. B. Weidemann and B. Hanel, *Luft- und Kältetechnik;* **24**, No. 3, 119-124 (1988).
8. R. A. Seban, M. M. Behnia, and K. E. Abreu, *Int. J. Heat Mass Transf.*, **21**, 1453-1458 (1978).
9. T. Mizushina, F. Ogina, H. Takeuchi, and H. Ikawa, *Wärme- und Stoffübertragung*, **16**, No. 1, 15-21 (1982).

RHEODYNAMICS AND EXCHANGE OF HEAT IN THE FLOW OF POLYMERIZING FLUIDS IN A CYLINDRICAL CHANNEL

Z. P. Shul'man, B. M. Khusid, É. V. Ivashkevich, V. B. Érenburg, and N. O. Vlasenko

UDC 532.135:541.64

We examine a method by which to study the rheokinetic factor in an investigation of the hydrodynamics and heat exchange of reactive oligomers.

The development of scientific foundations for chemical formation, i.e., of methods to produce composition materials through the utilization of reactive oligomers, requires analysis of the role played by the rheokinetic factor in the problems of hydrodynamics and convective heat exchange in rheologically complex reacting media. The flow of reactive oligomers is accompanied by polymerization which leads to an increase in molecular mass and correspondingly to an increase in viscosity, by several tens of orders. To calculate the thermohydraulic characteristics of the flow, it is essential that we know the kinetics involved in the change in composition viscosity, i.e., rheokinetics.

In order to study the role of the rheokinetic factor, we employ the method of space—time separation (STS) between the thermochemical and thermohydrodynamic states [1]. A nonmoving composition is hardened in a reservoir (the thermochemical stage). Neither the flow channel nor the liquid heat exchange are, for all intents and purposes, encumbered by the kinetics of polymerization (the thermohydrodynamic stage). The constant-pressure unit consists of an individually thermostatted reservoir and of a channel with identical or different temperatures. An ÉD-20 epoxy resin was used in the experiments in addition to a metaphenylene diamine hardener. The STS is achieved through special selection of regime parameters: $d_c/d_r \ll 1$ (d_r and d_c represent the diameters of the reservoir and the channel); $t_{stay} \sim t_{kin}$, $(t_{cha}/t_{res}) \approx 0.2$; $t_{res}/t_{kin} \ll 1$ (t_{stay}, t_{cha}, t_{res}, and t_{kin} represent the stay times within the reservoir, the time of motion through the channel, and the time of reservoir evacuations, in addition to the characteristic hardening time). The optimum regimes for the carrying out of these experiments in terms of the initial polymerization temperature, the ratio of reagents, and the length of time that the hardening composition remains within the reservoir, these were all determined from the condition of proximity of this process to the isothermal state. Thus, the initial process temperatures were 60, 65, and 67.5°C, the reagent ratios were assumed to be stoichiometric, while the stay time of the reacting mixture in the reservoir varied from 30 to 60 min. The effect of rheokinetics on convective heat exchange in a partially polymerized composition was investigated for the case of a nonisothermal flow through a round channel with a constant wall temperature of $T_w = 40$°C. The thermophysical characteristics of the composition were as follows: density ρ, thermal conductivity λ, thermal diffusivity a, in the range of 40-70°C, where they change only slightly as heating takes place [2]. They were therefore assumed to be constant and, on the average, equal to: $\lambda = 0.153$ W/(m·K); $\rho = 1.14 \cdot 10^3$ kg/m^3; and $a = 0.86 \cdot 10^{-7}$ m^2/sec.

With consideration of the chemical and rheological kinetics, we selected two stay times of the reacting mixture in the reservoir for the hardening composition,namely t = 30 and 35 min. These corresponded to the following depths of cnversoin: $\beta = 0.072$ and 0.088. Three fixed loads were used for each of these, and two of these, i.e., $\Delta P = 3.65 \cdot 10^4$ and $6.547 \cdot 10^4$ Pa, were reproduced for all stay times. The range of velocities 0.003-0.18 m/sec was chosen from the following conditions: a) the extent of the initial thermal segment is greater than the channel length (approximation of the thermally short channel); b) the flow time is sufficiently large to permit the mean-mass temperature metering probe to attain a steady regime at the inlet to the channel. Since the coefficient of thermal diffusivity for the epoxy compositions is small, the Peclet criterion (Pe), even at such low flow rates, amounts to $(0.6\text{-}5) \cdot 10^3$,

A. V. Lykov Institute of Heat and Mass Exchange, Academy of Sciences of the Belorussian SSR. Belorussian Polytechnic Institute, Minsk. "Altai" Scientific Production Association, Biisk. Translated from Inzhenerno-Fizicheskii Zhurnal, Vol. 60, No. 3, pp. 401-410, March, 1991. Original article submitted February 7, 1990.

 0022-0841/91/6003-0316$12.50